Nuclear Quadrupole Resonance of Tellurium Tetraiodide

Tsutomu OKUDA, Koji YAMADA, Yoshihiro FURUKAWA, and Hisao NEGITA

Department of Chemistry, Faculty of Science, Hiroshima University, Hiroshima 730

(Received May 22, 1975)

The nuclear quadrupole resonance (NQR) of ^{127}I in tellurium tetraiodide was observed, and the Zeeman effect on a single crystal was examined. Tellurium tetraiodide shows ten resonance lines in the frequency range from 195 to 260 MHz. From the analysis of the zero-splitting patterns, it has become apparent that tellurium tetraiodide crystals contain eight nonequivalent iodine atoms, two of which yield large asymmetry parameters (94.9% and 73.8%) and small quadrupole coupling constants (775.07 MHz and 929.55 MHz) at room temperature. These two may be assigned to the bridging iodine atoms, but they differ markedly from each other in the temperature dependences of e^2Qq/h and η. The other six iodine atoms have small η values and coupling constants of about 1600 MHz; they are assigned to the terminal atoms. From these results, it may be concluded that each tellurium atom has three terminal and two bridging iodine atoms.

The crystal structures of tellurium tetrachloride ($TeCl_4$)[1] and tellurium tetrabromide ($TeBr_4$)[2] are ionic and consist of tetramers $(TeX_3^+X^-)_4$ which have approximately the T_d symmetry. On the other hand, in the solid tellurium tetrafluoride (TeF_4)[3] each tellurium atom is surrounded by three terminal and two bridging atoms at the corners of a distorted square pyramid. These square pyramid units are linked by *cis* bridging into an endless chain. From the far-infrared spectrum of TeI_4,[4] it was concluded that TeI_4 has an ionic structure such as $TeI_3^+I^-$, because the spectrum is similar to those of SbI_3. According to the X-ray diffraction studies,[5] the crystal structure of TeI_4 belongs to an orthorhombic system with a space group P_{nma} or $Pn2_1a$, but its detailed structure has not been reported so far. In the NQR studies of $TeCl_4$ and $TeBr_4$,[6] six resonance lines were observed for both compounds; these lines were assigned to two species of TeX_3^+ (X=Cl, Br) ions. In this connection, we observed the ^{127}I NQR of TeI_4 and examined the Zeeman effect on a single crystal in order to determine the e^2Qq/h and η for each resonance line.

Experimental

The NQR spectrometer used in this experiment was a super-regenerative oscillator with frequency modulation, while the resonance frequencies were determined with a VHF signal generator and a frequency counter, TR-5578, from the Takeda Riken Co., Ltd. The Zeeman effect was examined by means of the zero-splitting cone method[7] on an oscilloscope at room temperature. The magnetic field of about 250 G was applied by means of a Helmholtz coil. The orientation of the magnetic field for the zero-splitting was determined by polar coordinates (Φ, Θ), where Φ and Θ are the azimuthal and polar angles respectively, in the coordinate system fixed to the sample. The single crystal of TeI_4 was grown by the Bridgman-Stockbarger method.

Results and Discussion

Zeeman Effect. As is shown in Table 1, ten resonance lines were observed in the frequency range from 195 to 260 MHz. As the nuclear spin of ^{127}I is equal to 5/2, a pair of NQR lines, ν_1 and ν_2, corresponding to the $\pm1/2\leftrightarrow\pm3/2$ and $\pm3/2\leftrightarrow\pm5/2$ transitions, are to be found for each kind of iodine atoms.[7] Therefore, the asymmetry parameter (η) and the quadrupole coupling constant (e^2Qq/h) can be derived from the frequency ratio, ν_1/ν_2. In the present compound, however, it is necessary to observe the Zeeman effect on each line in order to determine whether it is ν_1 or ν_2, and which ones form a pair, because the resonance lines distributed very widely.

In general, the zero-splitting cone can be expressed in the principal axis system of the efg tensor as follows:[7]

$$\sin^2\theta = \frac{A}{B+C\cos_2\phi} \qquad (1)$$

where θ and ϕ are, respectively the polar and azimuthal angles of the magnetic field which shows zero-splitting.

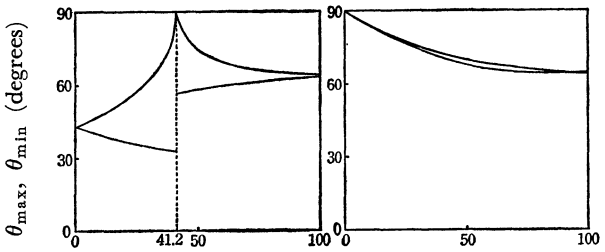

Fig. 1. Calculated maximum and minimum zero-splitting angles as a function of η for ν_1 and ν_2.

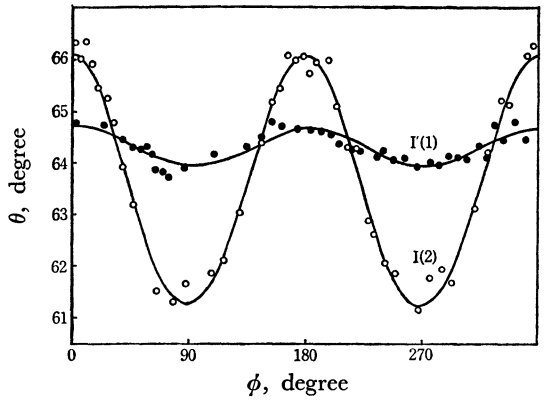

Fig. 2. Zeeman zero-splitting patterns of I'(1) and I(2) lines in the efg principal axis system.

Table 1. NQR parameters of TeI_4 (296 K and 77 K)

	ν_1 (MHz)		ν_2 (MHz)	η (%)[a]	η (%)[b]	e^2Qq/h (MHz)
I (1)	198.27 (198.67)[c]	I′ (1)	206.72 (212.78)	94.0±2.0 —	94.91 (91.70)	775.07 (793.66)
I (2)	205.23 (209.85)	I′ (2)	256.79 (259.15)	73.5±1.5 —	73.75 (75.23)	929.55 (940.44)
I (3)	228.52 (232.65)		—	3.2±0.5 —		1522.5 —
I (4)	234.82 (236.72)		—	5.6±0.5 —		1560.1 —
I (5)	242.75 (245.45)		—	5.6±0.5 —		1612.8 —
I (6)	243.27 (246.55)		—	1.2±0.5 —		1621.8 —
I (7)	250.86 (254.55)		—	1.4±0.5 —		1622.0 —
I (8)	252.35 (256.01)		—	2.9±0.5 —		1680.9 —

a) Obtained from the Zeeman effects. b) Obtained from the frequency ratio (ν_1/ν_2) using tabulated values of spin 5/2. c) The values in parentheses correspond to 77 K.

For the case of the 5/2 spin, A, B, and C can not be expressed in simple formulas when η is large. Hence, the maximum and minimum values of θ were calculated as a function of η for ν_1 and ν_2, as is shown in Fig. 1, according to the literature.[7,8] The zero-splitting patterns of I′(1) and I(2) lines are shown in Fig. 2 in the principal-axes system. The maximum and minimum values of θ for the zero-splitting patterns were obtained by the use of the least-squares method. These values were 66.1° and 61.3° for the I(2) pattern and 64.7° and 63.9° for that of I′(1). On the basis of these values, the I(2) line was assigned to ν_1, with $\eta=73.5\pm1.5\%$, and the corresponding ν_2 was observed at 256.79 MHz. On the other hand, the I′(1) pattern was assigned to ν_2, with $\eta=94.0\pm2.0\%$. The corresponding ν_1 was observed at 198.27 MHz, although this line was broad and weak compared with the others. The quadrupole coupling constants for these lines were calculated by the use of the tabulated eigenvalues of spin 5/2.

The I(3)~I(8) lines have approximately the same intensity for the powder sample, and from the zero-splitting patterns for the single crystal it becomes apparent that all these lines are ν_1 with small η values. For example, the zero-splitting patterns of the I(6) and I(7) lines are shown in Fig. 3. Therefore, η and e^2Qq/h can be calculated by means of the following equations:[7,9]

$$\eta = 17(\sin^2\theta_{max}-\sin^2\theta_{min})/24(\sin^2\theta_{max}+\sin^2\theta_{min}) \quad (2)$$

$$e^2Qq/h = 20\nu_1/3(1+1.0926\eta^2-0.6430\eta^4) \quad (3)$$

where θ_{max} and θ_{min} are the maximum and minimum zero-splitting angles. Table 1 shows the NQR parameters thus obtained. From these results it may be concluded that this crystal contains two nonequivalent TeI_4 molecules and that each tellurium atom is bonded to three terminal and two bridging iodine atoms. This configuration around the tellurium atom has a stronger resemblance to that of TeF_4 than to those of $TeCl_4$ and $TeBr_4$.

I(3) and I(6) yield two patterns of zero-splitting loci. On the other hand, for the I′(1), I(2), I(4), I(5), I(7), and I(8) lines only three patterns out of four were observed because one of the z-axis in each line was nearly parallel to the rf coil. From the symmetry of the observed patterns, three mutually perpendicular twofold axes were found within the limits

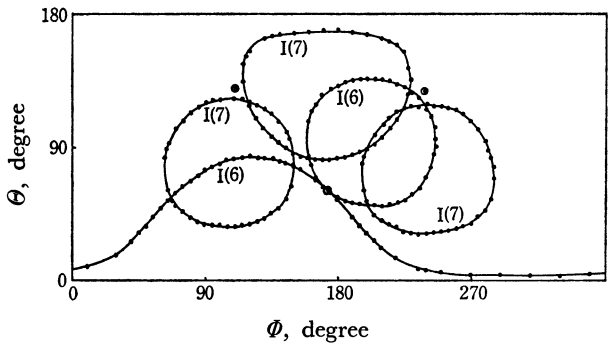

Fig. 3. Zero-splitting patterns of I(6) and I(7) lines in the coordinates fixed to the sample. Crystal axes of orthorhombic system are indicated by ⊙.

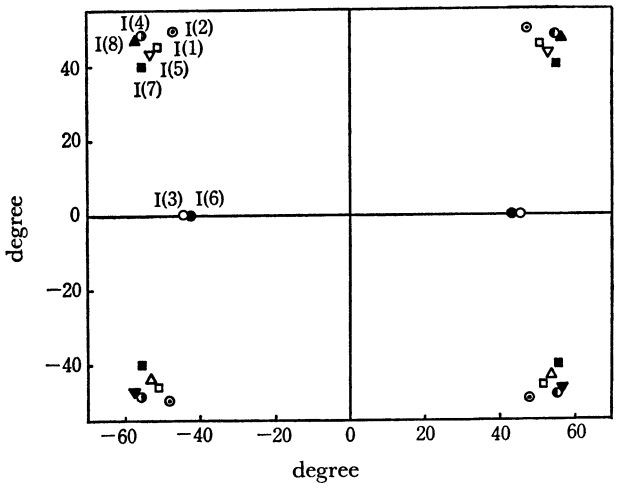

Fig. 4. Orientation of z-axes with respect to the crystal axes which are located at (0°, 0°), (90°, 0°), and (0°, 90°). In the case of I(2), y-axes are shown.

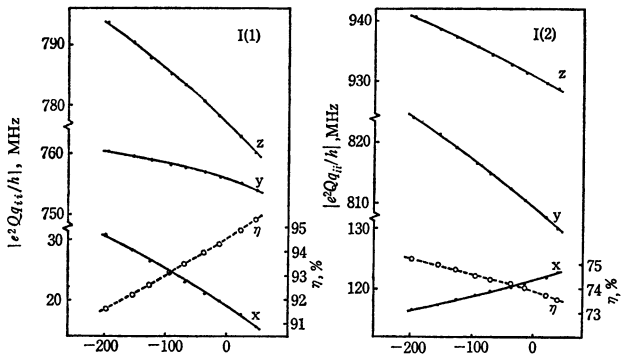

Fig. 5. Temperature dependence of quadrupole coupling constants for I(1) and I(2).

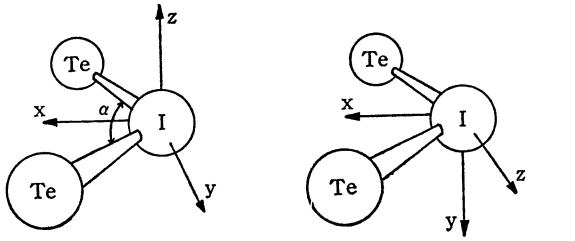

(a) $90° < \alpha < 109.5°$ (b) $109.5° < \alpha < 180°$

Fig. 6. Orientation of efg principal axis at a bridging iodine atom.

of experimental error. This finding suggests that the crystal is orthorhombic and that these three twofold axes correspond to the crystal axes.[10] Figure 4 shows the orientations of all the z-axes with respect to the crystal axes. In this figure, the three crystal axes are located at (0°, 0°), (90°, 0°), and (0°, 90°).

Temperature Dependences of the Quadrupole Coupling Constant for Bridging Iodines. Figure 5 shows the temperature dependences of $|e^2Qq_{zz}/h|$, $|e^2Qq_{yy}/h|$, and $|e^2Qq_{xx}/h|$ for I(1) and I(2). The principal values of the efg tensor can be expressed by:

$$\left.\begin{aligned} V_{zz} &= eq \\ V_{yy} &= -(1+\eta)eq/2 \\ V_{xx} &= -(1-\eta)eq/2 \end{aligned}\right\} \quad (4)$$

If the amplitudes of torsional oscillation about the x, y, and z axes are denoted by θ_x, θ_y, and θ_z respectively, the averaged principal values of the efg tensor can be expressed by the following equations:[11]

$$\left.\begin{aligned} V_{zz} &= eq_0\{1-\langle\theta_y^2\rangle(3-\eta_0)/2-\langle\theta_x^2\rangle(3+\eta_0)/2\} \\ V_{yy} &= eq_0\{-(1+\eta_0)/2+\langle\theta_z^2\rangle\eta_0+\langle\theta_x^2\rangle(3+\eta_0)/2\} \\ V_{xx} &= eq_0\{-(1-\eta_0)/2-\langle\theta_z^2\rangle\eta_0+\langle\theta_y^2\rangle(3-\eta_0)/2\} \end{aligned}\right\} \quad (5)$$

where q_0 and η_0 are the values in the static lattice and where $\langle\theta_i^2\rangle$ (i=x, y, and z) indicates the mean square amplitude of the oscillation about the i-axis. In the symmetrical bridging iodine, the principal axes of the efg tensor depend upon the bridging angle, as is shown in Fig. 6. It may be considered that the bridging iodine is more mobile in the direction perpendicular to the bridging plane than in that parallel to it. Therefore, we may assume that, in Model (a), the torsional oscillation about the y-axis contributes predominantly to the temperature dependence of the quadrupole coupling constant and the asymmetry parameter, whereas, in Model (b), the torsional oscillation about the z-axis contributes predominantly to the parameters. The temperature dependence of the I(1) atom can be interpreted satisfactorily by assuming $\langle\theta_x^2\rangle \approx \langle\theta_z^2\rangle < \langle\theta_y^2\rangle$ in Eq (5): this situation corresponds to Model (a). The positive temperature coefficient of η was also found for the bridging iodine in Al_2I_6 and Ga_2I_6.[12] These bridging iodine atoms have been supposed to have the principal axes of Model (a) by analogy with Al_2Br_6.[13] Therefore, the temperature dependence of the I(1) atom is mainly due to the characteristic torsional oscillation of the bridging iodine atom, as in those of Al_2I_6 and Ga_2I_6. Furthermore, the I(1) atom is supposed to have bonds such as those in Model (a).

On the other hand, the tendency of the I(2) atom can be roughly interpreted on the basis of Model (b) by assuming $\langle\theta_x^2\rangle \approx \langle\theta_y^2\rangle < \langle\theta_z^2\rangle$. However, as the quadrupole coupling constant of I(2) is fairly larger than that of I(1), it may be considered that I(2) is not so symmetrical in its bridging as I(1). Therefore, the variation in the electronic structure of the bridging iodine atom may also contribute to the temperature dependence of the quadrupole coupling constant.

References

1) B. Buss and B. Krebs, *Inorg. Chem.*, **10**, 2795 (1971).
2) C. B. Shoemaker and S. C. Abrahams, *Acta Crystallogr.*, **18**, 296 (1965).
3) A. J. Edwards and F. I. Hewaidy, *J. Chem. Soc., A*, **1968**, 2977.
4) N. N. Greenwood, B. P. Straughan, and A. E. Wilson, *J. Chem. Soc., A*, **1966**, 1479.
5) W. R. Blackmore, S. C. Abrahams, and J. Kalnajs, *Acta Crystallogr.*, **9**, 259 (1956). C. B. Shoemaker and S. C. Abrahams, *ibid.*, **18**, 296 (1965).
6) A. Schmitt and W. Zeil, *Z. Naturforsch., A*, **18**, 428 (1963). T. Okuda, K. Yamada, Y. Furukawa, and H. Negita, This Bulletin, **48**, 376 (1975).
7) T. P. Das and E. L. Hahn, "Nuclear Quadrupole Resonance Spectroscopy," Solid State Physics, Suppl. 1, Academic Press, New York (1957).
8) M. H. Cohen, *Phys. Rev.*, **96**, 1278 (1954).
9) I. P. Biryukov, M. G. Voronkov, and I. A. Safin, "Tables of Nuclear Quadrupole Resonance Frequencies," Israel, IPST Press (1969).
10) K. Shimomura, *J. Phys. Soc. Japan*, **12**, 652 (1957).
11) B. L. Barton, *J. Chem. Phys.*, **46**, 1553 (1967).
12) R. Barnes and S. Segel, *J. Chem. Phys.*, **25**, 578 (1956).
13) T. Okuda, H. Terao, O. Ege, and H. Negita, *ibid.*, **52**, 5489 (1970).